After-Fatigue Condition: A Novel Analysis Based on Surface EMG Signals

Van-Hieu Nguyen[1,*], Thien Van Luong[1], Mai Xuan Trang[1]
Gia Thien Luu[2], Philippe RAVIER[3], Olivier BUTTELLI[3]
[1]Faculty of Computer Science, Phenikaa University, Hanoi 12116, Vietnam
[2]Faculty of Information Technology, Ho Chi Minh City University of Technology, Ho Chi Minh, Viet Nam
[3]University of Orléans, France PRISME Laboratoire, 12 rue de Blois, BP 6744, 45067 Orléans, France
[*]E-mail: ngvan.hieu613@gmail.com Tel: +84378452566

Abstract—**This study introduces a novel muscle activation analysis based on surface electromyography (sEMG) signals to assess the after-fatigue condition of muscles. Previous studies have mainly focused on the pre-fatigue and post-fatigue conditions of muscles, but the after-fatigue condition has not been well explored. The proposed method analyzes muscle fatigue indicators at various maximal voluntary contraction (MVC) levels to compare the pre-fatigue, post-fatigue, and after-fatigue conditions using amplitude-based, spectral-based, and conduction velocity parameters. The contraction time of each MVC level is also analyzed with the same indicators. The results show that in the after-fatigue condition, muscle activation changes significantly in ways such as higher conduction velocity, power spectral density shifting to the right, and longer contraction time until exhaustion compared to the pre-fatigue and post-fatigue conditions. The results can provide a comprehensive and objective evaluation of muscle fatigue and recovery, which can be useful for clinical diagnosis, rehabilitation, and sports performance.**

I. Introduction

Surface electromyography (sEMG) is a non-invasive technique to measure the electrical activity of skeletal muscles. Surface EMG signals can provide valuable information about muscle fatigue, defined as the decrease of maximal force output to maintain or repeat tasks by muscles [1]. Muscle fatigue can affect the performance and health of muscles in various fields such as medicine, sports, rehabilitation, ergonomics, and human-machine interaction [2]–[4]. Therefore, assessing muscle fatigue based on sEMG signals is of great significance and especially interesting to researchers and health professionals.

Surface EMG signals are a valuable tool to evaluate muscle fatigue, and their applications in life and industrial fields are promising and diverse. However, assessing muscle fatigue based on sEMG is not a simple task because it involves many complex factors, such as muscle type, contraction type, electrode placement, signal processing method, and fatigue indices[5]. Surface EMG signals are often affected by noise from various sources, such as motion artifacts, skin perspiration, skin impedance, and electromagnetic interference [6], [7]. Therefore, robust and reliable methods are in demand to extract meaningful features from sEMG signals and to classify the states of muscles before, during, and after muscle fatigue. Feature extraction of sEMG signals is a method of extracting useful information from signals under different muscle conditions. Muscle fatigue is usually identified by the decrease of frequency domain indices and time-frequency domain indices and the increase of time domain indices. The traditional approach to acquiring sEMG signals is still commonly used in physiological and clinical studies, based on a pair of electrodes placed on the skin over the muscle. However, the acquired signal depends on the location, the distance between electrodes, the size of the electrode pair, and the location along the muscle fiber, which can lead to very different spectral characteristics and amplification [5], [6].

Initially, sEMG signal features can be divided into three domains: time domain, frequency domain, and time-frequency domain. However, in the past 40 years, a large number of parameters extracted from sEMG signals to evaluate muscle fatigue have been developed. Currently, sEMG features are divided into amplitude-based parameters, spectral-based parameters, non-linear parameters, and muscle fiber conduction velocity estimation (CV) [8], [9]. For the classical bipolar (bipolar) measurement method, using methods based on more than two electrodes arranged in series (linear array) allows collecting sEMG signals along the vertical or horizontal axis of the muscle [10]. A relatively recent approach includes using multiple electrode groups arranged in one- or two-dimensional arrays. In addition, the two-dimensional electrode array can be used to determine the distribution of sEMG amplitude and describe the spectrum over the entire skin area covering the muscle [11]. Multichannel sEMG signals also allow for more accurate and reliable estimation of CV [12].

Our research is based on previous studies that have used multichannel sEMG to analyze muscle activity at different MVC levels and during muscle fatigue. For example, reference [8], [13] investigated the power spectral density (PSD) of sEMG at various MVC levels. Reference [9] used a linear array sEMG to examine the relationship between CV and the shift of power spectral density over time with different load levels. However, the pre-fatigue condition has not been well investigated in these studies.

By analyzing the general fatigue indicators from self-supplied data according to pre-fatigue, post-fatigue, and after-fatigue conditions at different MVC levels and contraction times, we found a significant increase in MVC maintenance time at low levels. Therefore, with this study, we aim to achieve a deeper understanding of the mechanism of this finding and its impact on muscle activation.

II. Methods

A. Signal acquisition protocol and data pre-processing

The sEMG signals from all electrodes obtained from the MVC levels were digitally filtered (20Hz-400Hz) to reduce noise. Data collection on 10 healthy subjects including states: before muscle fatigue including 10%, 20%, 40%, 60%, 90% (MVC), during muscle fatigue 70%MVC, after muscle fatigue 10%MVC. Subjects were asked to maintain MVC levels for each state until exhaustion (Fig. 1. A). In the following sections, we implicitly understand 10MVC, 20MVC, 40MVC, 60MC, and 90MVC. If nothing else is described, it will be denoted for the state before muscle fatigue. 70MVC during muscle fatigue and 10MVC after muscle fatigue is clearly described.

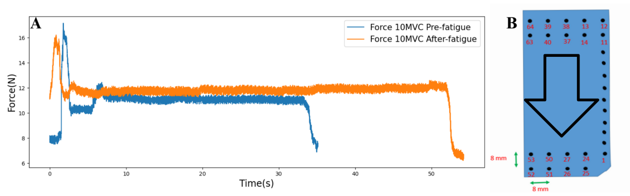

Fig. 1. A. Representation of the longer force's contraction time until exhausted. B. The sensor is used in signal acquisition.

B. Amplitude-based parameters

Root mean square (RMS) is the main parameter used to investigate the amplitude of the sEMG signal. The formula for RMS is as follows:

$$RMS = \sqrt{\frac{1}{n}\sum_{n} x_n^2}(\mu V) \tag{1}$$

where x_n are the values of the sEMG signal and n is the number of data samples. RMS is believed that during maximal isometric contractions, amplitude falls progressively, in parallel with the decrease in force [14].

C. Spectral-based parameters

Two characteristic frequencies that have been used to quantify changes in spectral content based on Fourier transform are the mean frequency (MNF) and the median frequency (MDF) of the power spectrum. [15].

MDF is calculated as follows:

$$MDF = \int_{f1}^{f_{median}} PS(f).df = \int_{f_{median}}^{f_2} PS(f).df(Hz) \tag{2}$$

MNF is calculated as follows:

$$MNF = \frac{\int_{f1}^{f2} f.PS(f).df}{\int_{f1}^{f2} PS(f).df}(Hz) \tag{3}$$

where PS(f) is the power spectrum calculated from the Fourier transform, f1 and f2 determine the lowest and highest frequency of the signal bandwidth, usually ranging from 20Hz to 400Hz. MDF and MNF are related to the change in conduction velocity and have been shown in isometric contractions that MNF will shift to lower frequencies during fatigue [16].

D. Estimate conduction velocity

Initially, the muscle's conduction velocity (CV) was calculated based on placing a series of electrodes along the muscle. However, this method has been proven biased in estimating CV because muscle fibers are not placed in a parallel plane. Moreover, electrodes placed on an undefined muscle domain can lead to misleading information [17]. Recently, multi-channel sEMG signals allowed more accurate estimation of CV both at the global level of the muscle and CV of individual motor units. Therefore, our study conducted CV estimation on multi-channel algorithms on selected signals. Three single differential sEMG signals were selected to remove the mean value. The algorithm calculated two double-differential sEMG signals and estimated the delay time between the two signals. After the delay time was calculated, CV was obtained by dividing the electrode distance by the delay time. The formula for calculating CV is as follows:

$$CV = \frac{d}{\theta} \tag{4}$$

where d is the distance between two electrodes, θ is the delay time between two electrodes. The algorithm is described in more detail in [18].

Conduction velocity is not only a mathematical index but also directly related to the properties of fiber membrane, fiber diameter, and contraction properties of the fiber. Measuring CV degradation is considered as the strongest indicator of muscle fatigue [19]. In addition, changes in the CV in muscle fatigue have a profound impact on the motor unit action potential waveform and therefore affect both amplitude parameters and spectral parameters extracted from sEMG [20], [21]. Previous studies have also shown that CV is reduced due to the consequences of local metabolic changes in active muscles, mainly due to H+ and K+ distribution in sarcolemma [22], [23].

E. Proposed method

In the analysis method, according to MVC levels, amplitude parameters and spectral parameters were calculated on the entire sEMG signal obtained, except for the noise part at the beginning and end of the signal. The MNF and RMS parameters obtained from each MVC level were averaged over all signals. The innervation zone was determined by visualizing the signals of the electrodes through a single differential filter (Fig. 2.).

The multichannel algorithm mentioned earlier estimated the conduction velocity (CV) with selected sEMG signals. The CV value was accepted if the correlation coefficient between

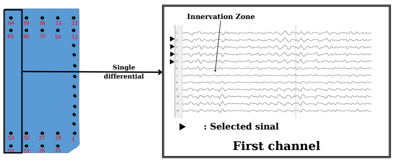

Fig. 2. Representation of Innervation zone and signals selection.

adjacent signals was more significant than 0.75. The estimated CV value of each MVC level was averaged over channels.

For the analysis method according to contraction time, each selected signal will be divided into intervals, spaced 1000ms and 500ms long. MNF and RMS obtained from each MVC level were averaged over all selected signals. The PSD representation of the signal was divided into three intervals, each with a length of 1000ms. "Onset" is taken at the beginning of the signal, "Middle" is taken in the middle of the signal, and "End" is taken at the end of the signal.

CV was calculated on each selected signal with segments 500ms long and spaced 1000ms apart. The CV value was accepted if the correlation coefficient between adjacent signals was more significant than 0.75. The estimated value of CV for each MVC level was averaged over channels.

III. Results

A. *Results from analysis of each MVC level*

We are interested in the shift of the power spectrum according to frequency. We represented the PSD in normalized units (Fig. 3. A). The frequency at the maximum power level of the MVC levels is approximately 15Hz, and this can help us preliminary predict how the average frequency of these MVC levels will shift (Fig. 3. E). Starting from 10MVC, it can be easily seen that 10MVC has a higher average frequency than other MVC levels before muscle fatigue, except for 20MVC. It can be explained that 20MVC requires more muscle force than 10MVC, the increasing the muscle force requirement before fatigue will coincide with the increase in amplitude and frequency shift (Fig. 3. D); this is consistent as shown in the report of [22]. The above conclusion is also proper for the difference between 60MVC and 90MVC; when going up to a higher MVC level, PSD tends to compress at a lower frequency. Therefore, the general trend of the average frequency of MVC levels before muscle fatigue will tend to decrease when going up to higher MVC levels. For the 70MVC level in a state of muscle fatigue, the force generated between 60MVC and 90MVC shows a powerful frequency shift when muscle fatigue, accompanied by a robust decrease of CV and RMS compared to other MVC levels before muscle fatigue. This is consistent with what we expect in a state of muscle fatigue.

Meanwhile, when we compare the 10MVC level before, and after muscle fatigue with each other, there has been an increase in all indicators in the post-fatigue condition. The frequency shift at 10MVC after muscle fatigue is a robust change (Fig. 5. A.), and the frequency of maximum power level shifts from approximately 15Hz to approximately 40Hz. This increase also comes with a surge in CV and MNF. However, lower of increasing in amplitude, we suggest this change as muscle recovery. These characteristics can be indicators for the recovery condition which need to consider in further research at higher MVC levels under the after-fatigue condition.

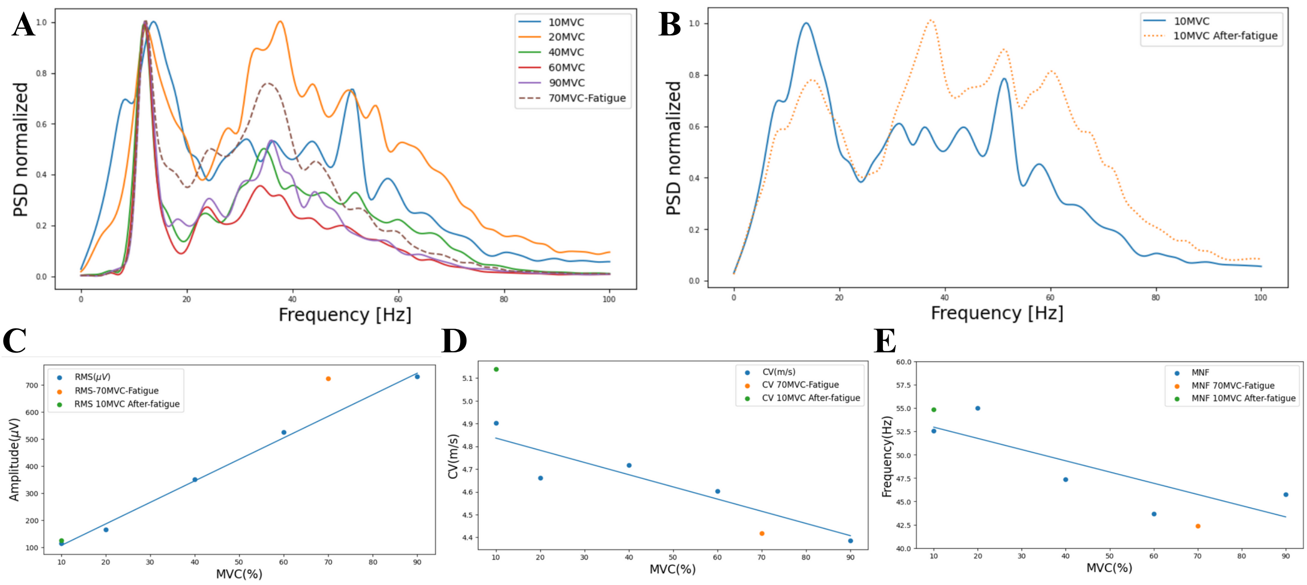

Fig. 3. A. PSD normalized each MVC level. B. PSD normalized of 10MVC pre-fatigue and after-fatigue. C. RMS each MVC level. D. CV each MVC level. E. MNF each MVC level

B. Results from analysis contraction time

The power spectrum of 10MVC before muscle fatigue over time (Fig. 4), we can preliminarily evaluate the change over time of the level of 10MVC is almost unchanged in terms of average frequency, increased relatively high in the middle of the signal. However, when observing the average frequency, amplitude, and CV, the change in the trend of these indicators is not apparent, in which CV of 20MVC has signs of slight muscle fatigue over time (Table I); this may have affected the power spectrum density of 20MVC that we mentioned in the analysis by MVC level.

Observing the 60MVC and 90MVC levels, we see an apparent change in power spectrum density over time. The closer to the end of the signal, the more we see the compression of PSD to the lower frequency domain. When observing parameters such as MNF, RMS, and CV for high MVC levels such as 90MVC that we described the slope change in Table I. The linear decrease of MNF and CV is apparent, accompanied by a high increase in RMS. This is also true for 70MVC in a muscle fatigue state. The result shows that fatigue increases over time and shows clearly that the higher the MVC level, the faster muscle fatigue occurs.

When comparing 10MVC pre-fatigue and 10MVC after-fatigue, we see a phenomenon opposite to other MVC levels. At the power spectrum density of 10MVC after muscle fatigue (Fig. 5.), we see a gradual shift to a higher frequency domain clearer over time. This partly explains the maintenance of muscle contraction time and shows that muscle activity after muscle fatigue at a low level, like 10MVC, seems to be less tired over time. Hen we look at parameters such as amplitude, frequency, and velocity, there is not much change in the frequency and amplitude of both states at this MVC level. However, when observing the CV of the 10MVC level after muscle fatigue over time, there was a slight increase over time. This partly explained the shift to the right of the frequency of 10MVC after muscle fatigue, and we hypothesized that there was reabsorption and distribution of ions such as H+ and K+ in the muscle membrane, leading to an increase in CV. This further proved the prolongation of the time to maintain muscle contraction at low MVC levels.

IV. Conclusions

The decline of CV, MNF, an increase of RMS, and a shift of power spectrum to lower frequency according to different MVC levels before and during muscle fatigue all provide results that we expect about the trend of muscle fatigue.

Regarding the significant increase in muscle contraction maintenance time at 10MVC level after muscle fatigue. We believe that this increase in time is related to the reabsorption and redistribution of ions after muscle fatigue. Because as mentioned earlier, the change of CV has a solid relationship to the change of metabolism at the cell membrane. The CV also has a significant impact on the amplitude parameters and spectrum parameters, shown in the increase of power spectrum density at higher frequencies and a slight increase in RMS and muscle force. However, this finding needs further investigation of the properties of the individual motor unit, such as firing rate, recruitment threshold, and synchronization.

TABLE I
PARAMETER'S SLOPE CHANGE OF EACH MVC LEVEL DURING CONTRACTION TIME

Parameters	MVC levels					
	10MVC	20MVC	40MVC	60MVC	90MVC	70MVC Fatigue	10 After-fatigue
MNF	0.101	0.016	-0.321	-0.466	-1.019	-0.64	0.007
RMS	-0.357	-0.051	7.987	15.417	22.376	21.093	-0.004
CV	-0.001	-0.013	-0.019	-0.026	-0.045	-0.054	0.003

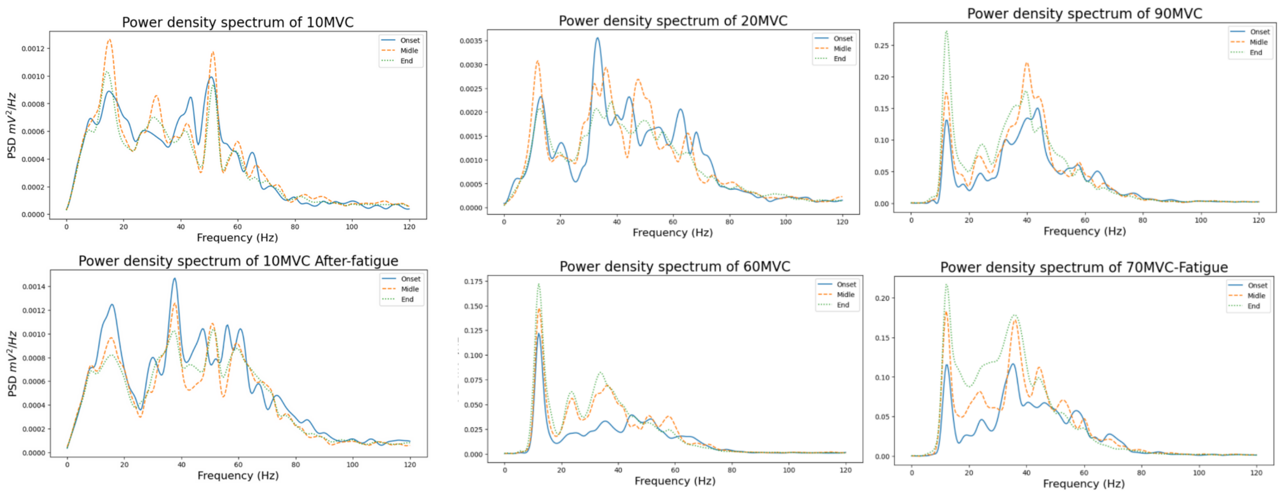

Fig. 4. Representation of the PSD shift during the contraction time.

B

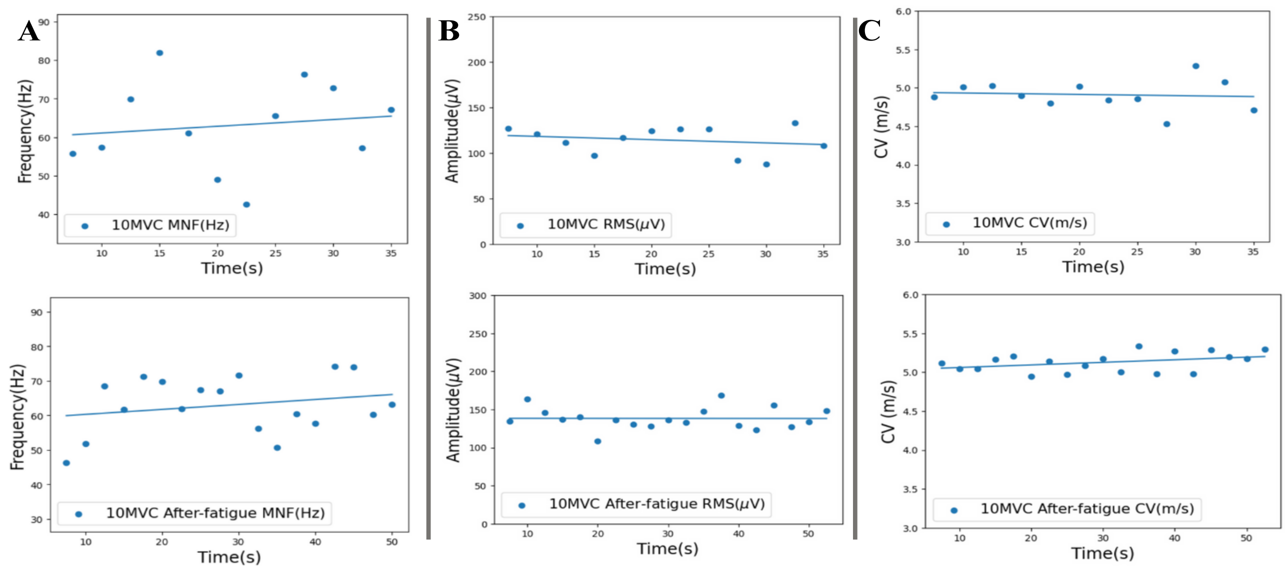

Fig. 5. A. MNF during contraction time of 10MVC pre-fatigue and after-fatigue. B. RMS during contraction time of 10MVC pre-fatigue and after-fatigue. C. CV during contraction time of 10MVC pre-fatigue and after-fatigue.

REFERENCES

[1] R. M. Enoka and J. Duchateau, "Muscle fatigue: What, why and how it influences muscle function," *The Journal of Physiology*, pp. 11–23, Jan. 2008.

[2] J. Reed and J. D. Bowen, "Principles of sports rehabilitation," *The Sports Medicine Resource Manual*, pp. 431–436, 2008.

[3] J. Sun, G. Liu, Y. Sun, K. Lin, Z. Zhou, and J. Cai, "Application of surface electromyography in exercise fatigue: A review," *Frontiers in Systems Neuroscience*, vol. 16, p. 893 275, Aug. 2022. [Online]. Available: https://www.ncbi.nlm.nih.gov/pmc/articles/PMC9406287/.

[4] B. Katirji, "Routine clinical electromyography," Sep. 2018.

[5] F. Bai, T. M. Lubecki, C.-M. Chew, and C. H. Teo, "Novel time-frequency approach for muscle fatigue detection based on semg," Nov. 2012.

[6] Z. Xiaoqi, L. Yun, and Z. Qianxiang, "Evaluation of muscle fatigue based on surface electromyography and subjective assessment," pp. 2003–2006, Jan. 2013. DOI: 10.1007/978-3-642-29305-4_526.

[7] M. B. I. Reaz, M. S. Hussain, and F. Mohd-Yasin, "Techniques of emg signal analysis: Detection, processing, classification and applications (correction)," *Biological Procedures Online*, vol. 8, pp. 163–163, Dec. 2006. DOI: 10.1251/bpo124.

[8] A. J. Lloyd, "Surface electromyography during sustained isometric contractions.," *Journal of Applied Physiology*, vol. 30, pp. 713–719, May 1971. DOI: 10.1152/jappl.1971.30.5.713.

[9] T. Sadoyama, T. Masuda, and H. Miyano, "Relationships between muscle fibre conduction velocity and frequency parameters of surface emg during sustained contraction," *European Journal of Applied Physiology and Occupational Physiology*, vol. 51, pp. 247–256, Aug. 1983. DOI: 10.1007/bf00455188.

[10] R. Merletti, D. Farina, and M. Gazzoni, "The linear electrode array: A useful tool with many applications," *Journal of Electromyography and Kinesiology*, vol. 13, pp. 37–47, Feb. 2003. DOI: 10.1016/s1050-6411(02)00082-2.

[11] D. Falla and D. Farina, "Periodic increases in force during sustained contraction reduce fatigue and facilitate spatial redistribution of trapezius muscle activity," *Experimental Brain Research*, vol. 182, pp. 99–107, May 2007. DOI: 10.1007/s00221-007-0974-4.

[12] M. Beretta-Piccoli, G. D'Antona, C. Zampella, M. Barbero, R. Clijsen, and C. Cescon, "Test-retest reliability of muscle fiber conduction velocity and fractal dimension of surface emg during isometric contractions," vol. 38, pp. 616–630, Mar. 2017. DOI: 10.1088/1361-6579/aa614c.

[13] S. Nagata, A. B. Arsenault, D. Gagnon, G. Smyth, and P. A. Mathieu, "Emg power spectrum as a measure of muscular fatigue at different levels of contraction," *Medical Biological Engineering Computing*, vol. 28, pp. 374–378, Jul. 1990. DOI: 10.1007/BF02446157. [Online]. Available: https://pubmed.ncbi.nlm.nih.gov/2246938/.

[14] M. Beretta-Piccoli, C. Cescon, and G. D'Antona, "Evaluation of performance fatigability through surface emg in health and muscle disease: State of the art," *Arab Journal of Basic and Applied Sciences*, vol. 28, pp. 21–40, Dec. 2020. DOI: 10.1080/25765299.2020.1862985.

[15] M. González-Izal, A. Malanda, E. Gorostiaga, and M. Izquierdo, "Electromyographic models to assess muscle fatigue," *Journal of Electromyography and Kinesiology*, vol. 22, pp. 501–512, Aug. 2012. DOI: 10.1016/j.jelekin.2012.02.019.

[16] R. Merletti and L. R. Lo Conte, "Surface emg signal processing during isometric contractions," *Journal of Electromyography and Kinesiology*, vol. 7, pp. 241–250, Dec. 1997. DOI: 10.1016/s1050-6411(97)00010-2.

[17] R. Merletti, *Surface Electromyography : Physiology, Engineering, and Applications*. Apr. 2016. DOI: 10.1002/9781119082934.

[18] K. C. McGill and L. J. Dorfman, "High-resolution alignment of sampled waveforms," vol. BME-31, pp. 462–468, Jun. 1984. DOI: 10.1109/tbme.1984.325413.

[19] A. J. Fuglevand, K. M. Zackowski, K. A. Huey, and R. M. Enoka, "Impairment of neuromuscular propagation during human fatiguing contractions at submaximal forces.," *The Journal of Physiology*, vol. 460, pp. 549–572, Jan. 1993. DOI: 10.1113/jphysiol.1993.sp019486.

[20] D. A. Gabriel and G. Kamen, "Experimental and modeling investigation of spectral compression of biceps brachii semg activity with increasing force levels," *Journal of Electromyography and Kinesiology*, vol. 19, pp. 437–448, Jun. 2009. DOI: 10.1016/j.jelekin.2007.10.009.

[21] L. R. Brody, M. Pollock, S. Roy, C. D. Luca, and B. R. Celli, "Ph-induced effects on median frequency and conduction velocity of the myoelectric signal," vol. 71, pp. 1878–1885, Nov. 1991. DOI: 10.1152/jappl.1991.71.5.1878.

[22] N. Dimitrova and G. Dimitrov, "Interpretation of emg changes with fatigue: Facts, pitfalls, and fallacies," *Journal of Electromyography and Kinesiology*, vol. 13, pp. 13–36, Feb. 2003. DOI: 10.1016/s1050-6411(02)00083-4.

[23] T. Masuda, H. Miyano, and T. Sadoyama, "The propagation of motor unit action potential and the location of neuromuscular junction investigated by surface electrode arrays," *Electroencephalography and Clinical Neurophysiology*, vol. 55, pp. 594–600, May 1983. DOI: 10.1016/0013-4694(83)90171-2.